

Mutations in *TNFRSF13B* encoding TACI are associated with common variable immunodeficiency in humans

U Salzer¹, H M Chapel², A D B Webster³, Q Pan-Hammarström⁴, A Schmitt-Graeff⁵, M Schlesier¹, H H Peter¹, J K Rockstroh⁶, P Schneider⁷, A A Schäffer⁸, L Hammarström⁴ & B Grimbacher¹

The functional interaction of BAFF and APRIL with TNF receptor superfamily members BAFFR, TACI and BCMA is crucial for development and maintenance of humoral immunity in mice and humans. Using a candidate gene approach, we identified homozygous and heterozygous mutations in *TNFRSF13B*, encoding TACI, in 13 individuals with common variable immunodeficiency. Homozygosity with respect to mutations causing the amino acid substitutions S144X and C104R abrogated APRIL binding and resulted in loss of TACI function, as evidenced by impaired proliferative response to IgM-APRIL costimulation and defective class switch recombination induced by IL-10 and APRIL or BAFF. Family members heterozygous with respect to the C104R mutation and individuals with sporadic common variable immunodeficiency who were heterozygous with respect to the amino acid substitutions A181E, S194X and R202H had humoral immunodeficiency. Although signs of autoimmunity and lymphoproliferation are evident, the human phenotype differs from that of the *Tnfrsf13b*^{-/-} mouse model.

Tumor necrosis factor (TNF)-like receptors are members of a superfamily of genes that transduce key signals to regulate both survival and apoptosis of immune cells. BAFF (B cell-activating factor, also called BLyS, THANK, TALL-1 and zTNF4; encoded by *TNFSF13B*) binds three TNF-like receptors selectively expressed on B cells called BAFFR (BAFF receptor, encoded by *TNFRSF13C*), TACI (transmembrane activator and CAML interactor, encoded by *TNFRSF13B*) and BCMA (B cell maturation protein A, encoded by *TNFRSF17*)^{1,2}. BAFF is expressed by macrophages and dendritic cells and provides a key survival signal for the maturation of peripheral B cells through BAFFR; the role of BAFF signaling through TACI and BCMA is less obvious^{1,2}. TACI is expressed on peripheral B cells, with highest expression found on the CD27⁺ B-cell subset³, whereas BCMA expression is restricted to plasmablasts and tonsillar germinal center B cells^{3,4}.

TACI and BCMA bind not only BAFF but also a second ligand called APRIL (a proliferation-inducing ligand, encoded by *TNFSF13*)⁵. APRIL-deficient mice have normal immunity⁶ apart from an impaired ability to induce class switching to IgA⁷. Functional studies propose a role for APRIL in T cell-independent class switch recombination (CSR)⁸, which is mediated, at least partly, by the interaction of APRIL with TACI⁹.

BAFF-deficient mice have fewer peripheral B cells and impaired T cell-dependent and -independent antibody responses¹⁰. BAFFR-deficient mice are similar but less severely compromised in their

immunophenotype¹¹, as they are still able to mount robust antibody responses against T cell-independent antigens¹², indicating that these may be mediated by TACI. A severe impairment of T cell-independent immune responses to polysaccharide antigens of encapsulated bacteria like *Streptococcus pneumoniae* in *Tnfrsf13b*^{-/-} mice further supports this finding¹³. In addition to this humoral immunodeficiency, *Tnfrsf13b*^{-/-} mice develop a lymphoproliferative disorder, evidenced by enlarged spleens and lymph nodes and development of lymphoma in up to 15% of mice¹⁴ and signs of a severe autoimmune disease with high titers of autoantibodies and a fatal nephritis^{14,15}. This coincidence of autoimmunity, lymphoproliferation and immunodeficiency is often seen in human individuals with common variable immunodeficiency (CVID)¹⁶, leading us to investigate *TNFRSF13B* as a candidate for involvement in CVID.

CVID (OMIM #240500) is diagnosed on the basis of an impaired ability to produce specific antibodies after vaccination or exposure, markedly reduced serum levels of IgG, IgA and (frequently) IgM and exclusion of other causes for antibody deficiency¹⁶. CVID has an estimated prevalence of 1 in 25,000 in Europeans and is the most prevalent human primary immunodeficiency requiring medical attention. Most cases of CVID are sporadic, but at least 10% are familial, with a predominance of autosomal dominant over autosomal recessive inheritance¹⁷. Many families have been identified with CVID and selective IgA deficiency in closely related individuals, suggesting that there might be a common genetic basis for these two disease entities¹⁸.

¹Division of Rheumatology and Clinical Immunology, Medical Center, University Hospital, Hugstetterstr. 55, 79106 Freiburg, Germany. ²Department of Immunology, Oxford Radcliffe Hospitals, Oxford, UK. ³Department of Clinical Immunology, Royal Free Hospital, London, UK. ⁴Division of Clinical Immunology, Karolinska Institute at Huddinge, Stockholm, Sweden. ⁵Institute of Pathology, University of Freiburg, Germany. ⁶Medizinische Universitätsklinik I, Bonn, Germany. ⁷Department of Biochemistry, University of Lausanne, Switzerland. ⁸National Center for Biotechnology Information, National Institutes of Health, Department of Health and Human Services, Bethesda, Maryland, USA. Correspondence should be addressed to B.G. (grimbacher@medizin.uni-freiburg.de).

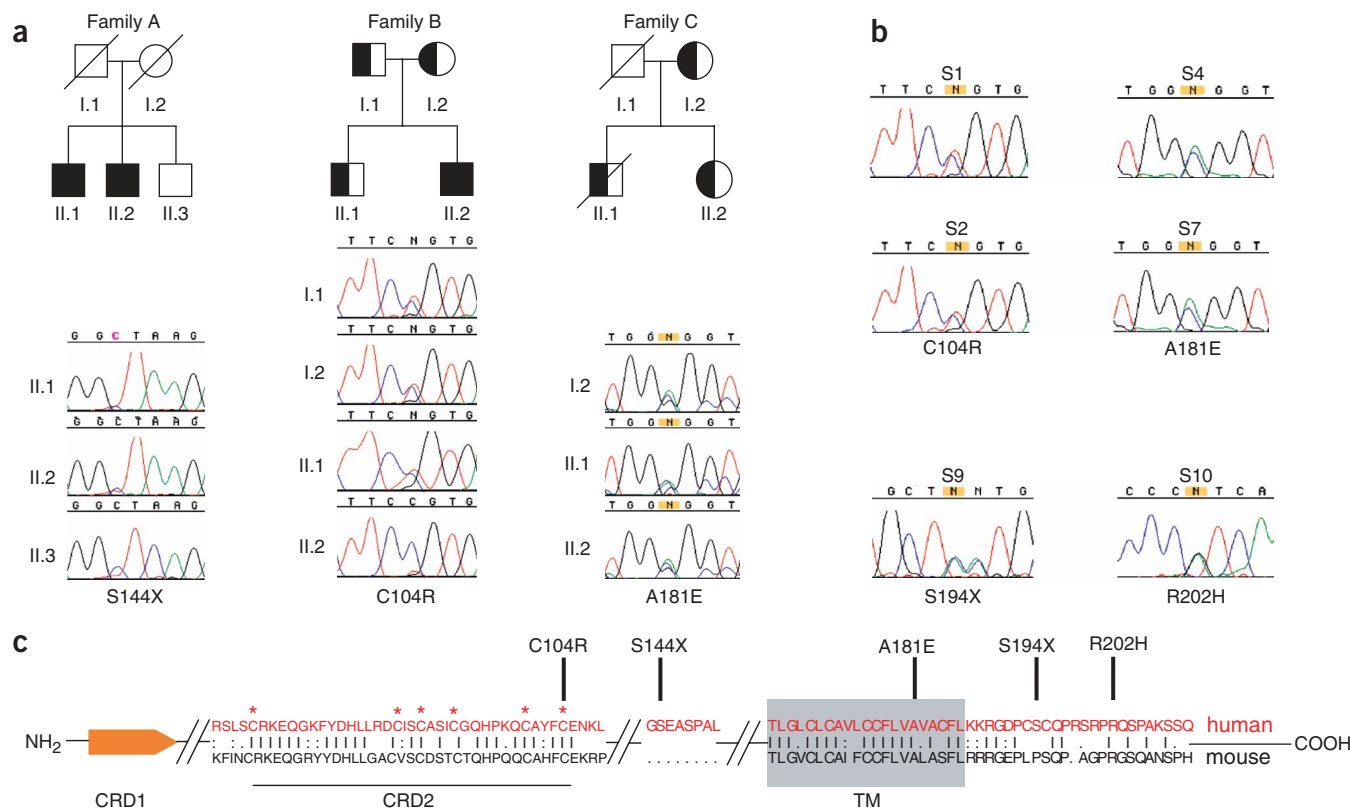


Figure 1 TAC1 mutations in CVID. **(a)** Mutations in *TNFRSF13B* in three families with CVID. Circles represent females; squares, males; filled symbols, homozygous individuals; half-filled symbols, heterozygous individuals; slashes, deceased individuals. For family A, the homozygous 444C→A transversion in *TNFRSF13B* mRNA (resulting in the amino acid mutation S144X) in individuals II.1 and II.2 is shown. Family B has the 323T→C transition (resulting in the amino acid substitution C104R) in a homozygous state in individual II.2 and in a heterozygous state in all other family members. Family C has the heterozygous 555C→A transversion (resulting in the amino acid substitution A181E) in individuals I.2, II.1 and II.2. **(b)** Mutations in *TNFRSF13B* in individuals with sporadic CVID. In individuals S1 and S2, the heterozygous 323T→C transition (resulting in the amino acid substitution C104R) is observed. In individual S9, two consecutive C→A transversions at positions 594 and 595 (resulting in the amino acid mutation S194X) are shown. Individuals S4 and S7 are heterozygous with respect to the 555C→A transversion (resulting in the amino acid substitution A181E). In individual S10, the heterozygous 618G→A transition (resulting in the amino acid substitution R202H) was found. **(c)** Scheme of the domain structure of *TNFRSF13B* with the human and mouse TAC1 sequences aligned. The position of the mutations are indicated. CRD, cysteine rich domain; TM, transmembrane region. Asterisks mark the locations of cysteine residues.

CVID is characterized by recurrent bacterial infections and is complicated by autoimmune manifestations in up to 20% of affected individuals and lymphoproliferation (splenomegaly) in approximately one-third¹⁶.

We recently showed that CVID might be a monogenic disorder in some families with autosomal recessive CVID, as ~2% of the cases are caused by homozygous mutations in the inducible costimulator of activated T cells (*ICOS*)^{19,20}. Here we show that an additional 5–10% of CVID cases carry at least one germline mutation in *TNFRSF13B*.

RESULTS

Sequencing *TNFRSF13B* in individuals with CVID

We screened 162 unrelated individuals with CVID for mutations in *TNFRSF13B*, including 135 'sporadic' cases and 27 index individuals with CVID from families with multiple cases of a humoral immunodeficiency. In these 27 multicase families, we identified three families that each had a different defect in *TNFRSF13B* (Fig. 1).

In family A, we observed the nonsense mutation S144X in the stalk region of TAC1. Both affected individuals (individuals A.II.1 and A.II.2) were homozygous with respect to the mutation; their unaffected sibling (A.II.3) was homozygous with respect to the wild-type

sequence (Fig. 1a). FACS analysis of peripheral blood lymphocytes from individual A.II.1 showed 8% peripheral B cells, but TAC1 expression could not be detected on Epstein-Barr virus (EBV)-transformed cell lines (Fig. 2a) or peripheral blood mononuclear cells (PBMCs; Supplementary Fig. 1 online).

Because the mutation S144X might result in a truncated TAC1 protein, possibly acting as a decoy receptor, we tested by ELISA whether the sera of individuals A.II.1 and A.II.2 (as well as individuals B.II.2, S4, S9 and S10) contained soluble TAC1. We were unable to detect a substantial amount of soluble TAC1 in the serum of individuals or controls. The cell lysate of an EBV-derived cell line from individual A.II.2 was also negative for TAC1 expression, whereas TAC1 was detected in the control (Supplementary Fig. 2 online). In addition, RT-PCR analysis detected no *TNFRSF13B*-specific mRNA in PBMCs from individuals A.II.1 and A.II.2 but did detect *TNFRSF13B* mRNA in controls (Fig. 2b). In addition, the *TNFRSF13B* mRNA levels were severely reduced in EBV-derived cells from individual A.II.2 compared with those in cells from individual B.II.2 and the healthy control, whereas *TNFRSF17* (*BCMA*) and *TNFRSF13C* (*BAFFR*) mRNAs were equally expressed in affected individuals and the control (Fig. 2c).

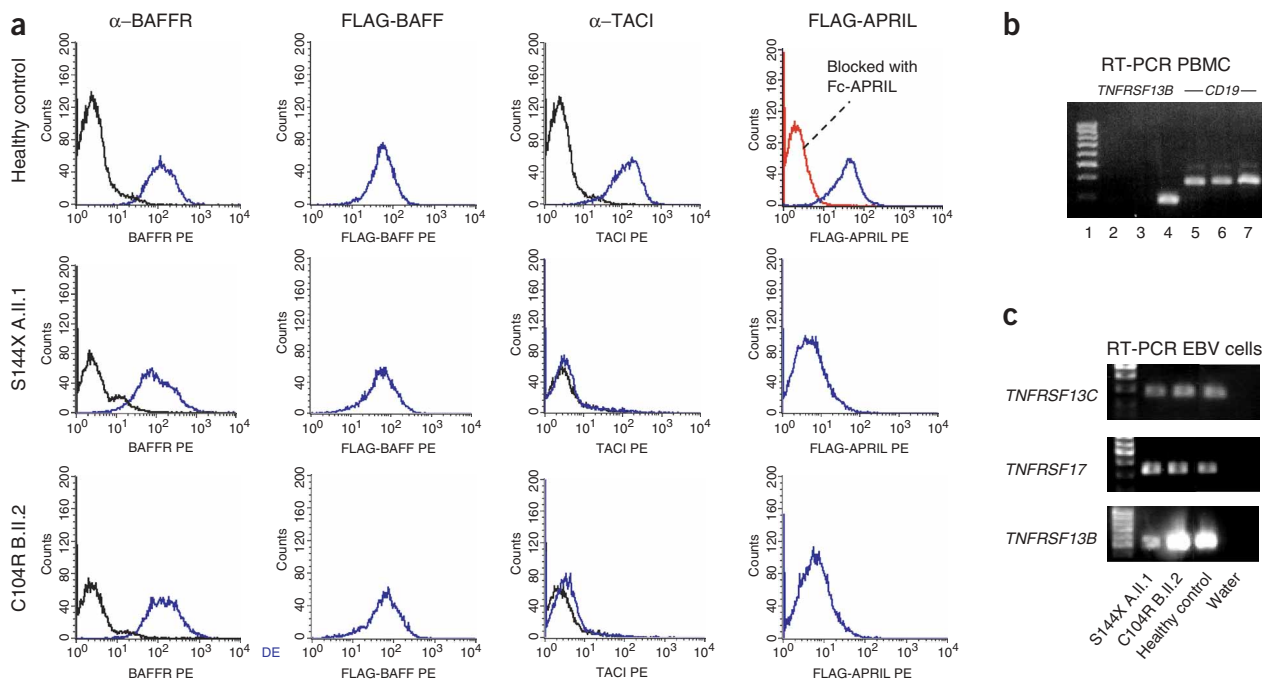


Figure 2 TAC1 deficiency impairs APRIL binding. **(a)** Expression of TAC1 and BAFFR and binding of APRIL and BAFF in EBV-transformed cell lines of individuals with the S144X and C104R mutations were tested. Black lines indicate isotype controls for antibody staining; blue lines show staining with antibodies to BAFFR or to TAC1 or with FLAG-BAFF and FLAG-APRIL. In individuals A.II.1 and B.II.2, BAFFR expression and BAFF binding was unaffected but binding of APRIL and 1A1 antibody to TAC1 was abrogated. The specificity of binding of FLAG-APRIL was shown by preincubation of healthy control B cells with Fc-APRIL (red line). **(b)** Analysis of *TNFRSF13B* mRNA expression in family A by RT-PCR. Lane 1, 100-bp marker; lanes 2 and 5, individual A.II.2; lanes 3 and 6, individual A.II.1; lanes 4 and 7, healthy control; lanes 2–4, TAC1; lanes 5–7, CD19 as a control for cDNA quality. The RT-PCR analysis shows absence of *TNFRSF13B* mRNA in individuals A.II.1 and A.II.2. **(c)** Analysis of *TNFRSF13C*, *TNFRSF17* and *TNFRSF13B* expression by RT-PCR in EBV-transformed cell lines of individuals with TAC1 deficiency. *TNFRSF13C* and *TNFRSF17* were expressed in individuals A.II.1 and B.II.2 at levels comparable to that observed in healthy controls, but *TNFRSF13B* mRNA expression was severely reduced in EBV-transformed cell lines of individual A.II.1.

The two affected individuals in family A were hypogammaglobulinemic. The index individual (individual A.II.2) suffered from recurrent otitis media at 9 years of age, was diagnosed as having CVID at 16 years of age after having pneumonia with a serum IgG of 2 g l^{-1} and then started regular immunoglobulin replacement therapy (Table 1). He had hepatosplenomegaly, and the spleen was surgically removed when he was 19 years of age because lymphoma was suspected. The histology of the spleen was normal. His brother (individual A.II.1) was found to have hypogammaglobulinemia (IgG of 4.1 g l^{-1} , normal range is $7\text{--}16 \text{ g l}^{-1}$; IgA of 0.2 g l^{-1} , normal range is $0.7\text{--}4.0 \text{ g l}^{-1}$; and IgM of 0.4 g l^{-1} , normal range is $0.4\text{--}2.3 \text{ g l}^{-1}$) during screening of the proband's relatives. He had never been susceptible to infections and had no splenomegaly but had an elevated circulating lymphocyte count ($4.77 \times 10^9 \text{ cells l}^{-1}$, normal range is $1.2\text{--}3.5 \times 10^9 \text{ cells l}^{-1}$) due to raised numbers of B cells and CD8⁺ T cells.

The mutation in family B affects a conserved cysteine residue (C104R) in the extracellular domain of TAC1. Individual B.II.2 was homozygous with respect to the mutation, his parents and sibling were heterozygous with respect to the same mutation (Fig. 1a). Cys104 forms a disulfide bond with Cys93 and participates in the maintenance of the second cysteine-rich domain of TAC1²¹. Staining of peripheral B cells or EBV-transformed B cells from individual B.II.2 with the TAC1 antibody 1A1 showed profoundly reduced surface expression (Fig. 2a and Supplementary Fig. 1 online).

The phenotype of the homozygous index individual B.II.2 included hypogammaglobulinemia, recurrent infections of the respiratory and gastrointestinal tracts and splenomegaly at 16 years of age. Notably, he

had a severe EBV-associated disease at 15 months of age. This episode was characterized by fatigue, weight loss and splenomegaly. Despite his profound hypogammaglobulinemia at that time, his serology was positive for EBV. X-linked lymphoproliferative syndrome was excluded by sequencing the gene *SH2D1A*. The three heterozygous carriers in family B presented with milder clinical phenotypes and reduced IgM levels (0.33, 0.31 and 0.38; normal range is $0.4\text{--}2.3 \text{ g l}^{-1}$) and low IgA levels (0.76, 0.61 and 1.24; normal range is $0.7\text{--}4.0 \text{ g l}^{-1}$).

In family C, we detected a heterozygous mutation leading to the amino acid substitution A181E (Fig. 1a) in the transmembrane region of TAC1. The index individual C.II.1 suffered from recurrent pneumonia, otitis and a chronic *Haemophilus influenzae* infection of the sinuses and upper respiratory tract. Other clinical manifestations included recurrent diarrhea, a therapy-resistant *Herpes zoster* infection, condylomata and enlarged peripheral lymph nodes. Two years later, individual C.II.1 died of a tonsillar carcinoma of epithelial origin. His sister, as well as her two sons (data not shown), all heterozygous with respect to the mutation, have IgA deficiency and suffer from recurrent infections.

Screening of 135 individuals with sporadic CVID identified 10 individuals carrying four different heterozygous mutations in *TNFRSF13B*. Three mutations led to nonconservative amino acid substitutions at residues that are conserved between mouse and human; the fourth is a nonsense mutation. Two individuals with sporadic CVID also carried the C104R mutation. Five individuals were heterozygous with respect to a mutation in the transmembrane region (A181E). We also identified one affected individual who was

homozygous with respect to this mutation. Finally, we identified two individuals with mutations in the intracellular C-terminal part of the protein, R202H and S194X (Fig. 1b). The mutations C104R, A181E and S194X did not result in impaired TACI expression in the heterozygous state (Supplementary Fig. 1 online). FACS analysis of EBV-derived cells from individuals A.II.1, B.II.2, S7 and S9 showed normal surface expression of BAFFR (Supplementary Fig. 1 online).

We did not find the cDNA substitutions resulting in the mutations C104R, A181E and R202H in databases of known polymorphisms using SNPPer²². All three missense changes are predicted, by sequence analysis using SIFT, to affect function²³. Sequencing of *TNFRSF13B* in 100 healthy individuals did not detect any of the five variants, suggesting that they are disease-associated mutations. In a second, larger survey, we found the A181E substitution in a heterozygous state in only 1 of 674 alleles of population-based controls checked by mass spectrometry, showing that the higher frequency in individuals with sporadic CVID (7 of 270 alleles) is statistically significant ($P < 0.001$, χ^2 test). Two known *TNFRSF13B* polymorphisms, resulting in the amino acid substitutions T27T and S277S, and two previously unpublished rare polymorphisms, R72H and V220A, were detected at similar frequencies among the CVID and control cohorts.

C104R or S144X homozygosity abrogates APRIL binding

To assess the binding capacity of B cells from individuals with CVID to their ligands BAFF and APRIL, we stained EBV-transformed B cell lines of individuals A.II.1 and B.II.2 with FLAG-tagged APRIL or FLAG-tagged BAFF. APRIL binding was severely compromised in both individuals, whereas BAFF binding was unaltered, reflecting normal BAFFR expression (Fig. 2a). The specificity of APRIL binding was shown by competition with APRIL carrying a different tag (Fc) in a healthy control (Fig. 2a).

C104R impairs proliferative response to IgM-APRIL

To assess the effect of TACI mutations on B-cell proliferation, we first isolated CD19⁺ cells from seven individuals with mutations in *TNFRSF13B* and stimulated them with antibody to IgM, with antibody to IgM plus interleukin-2 (IL-2), with antibody to CD40 or with

antibody to CD40 plus IL-4. In all instances, CD19⁺ B cells proliferated normally (Supplementary Fig. 3 online).

In a second set of experiments, we stimulated enriched B cells of individual B.II.2 and a healthy control with IgM alone, with IgM plus recombinant IL-2 or with IgM plus soluble FLAG-tagged APRIL, cross-linked with an antibody to FLAG²⁴. In the healthy control, B cells responded to IgM-APRIL costimulation with a two- to threefold increase of proliferation relative to the response stimulated by IgM alone, reaching levels comparable to that stimulated by IgM plus IL-2 (Fig. 3a). In individual B.II.2 (homozygous with respect to the mutation C104R), B cells responded well to IgM plus IL-2 but did not respond to IgM-APRIL costimulation (Fig. 3a). Therefore, B-cell proliferation in response to IgM-APRIL costimulation is selectively impaired.

APRIL and BAFF do not induce CSR in TACI deficiency

In the presence of appropriate cytokines, APRIL and BAFF induce CD40-independent CSR⁸. To study whether mutations of TACI influence the ability of cells to switch to IgG, we stimulated PBMCs from individuals with CVID and controls with recombinant CD40L, APRIL or BAFF, in the presence of IL-10. We determined the rates of $I\gamma$ -C μ germline transcription and formation of $I\gamma$ -C μ circle transcripts and the amount of IgG secreted in the culture supernatants.

After normalization of the transcription rate, $I\gamma$ -C μ germline transcripts were induced two- to fourfold by CD40L, APRIL or BAFF in cells from a normal blood donor (Fig. 3b). In contrast, in cells from individual B.II.2, $I\gamma$ -C μ germline transcripts were upregulated only by CD40L (by four- to eightfold) and not by APRIL or BAFF (Fig. 3b).

We detected weak expression of $I\gamma$ -C μ circle transcripts in the unstimulated control cells. This expression was upregulated by CD40L, APRIL and BAFF (Fig. 3b). We detected small amounts of $I\gamma$ -C μ circle transcripts in unstimulated and in CD40L- or APRIL-stimulated cells from individual B.II.2 (Fig. 3b) but no upregulation by either stimulus.

We then determined the ability of B cells from the control individual and from individuals with CVID to secrete IgG in response

Figure 3 Proliferation and CSR in response to APRIL and BAFF.

(a) Proliferation of purified B cells in response to IgM-APRIL costimulation. Proliferation of enriched B cells of individual B.II.2 in response to antibody to IgM, antibody to IgM plus IL-2 or antibody to IgM plus supernatants of 293T cells transfected with plasmids expressing soluble APRIL is shown. B cells from an individual with TACI deficiency (B.II.2, C104R) and a healthy control proliferated equally after stimulation with IgM and IgM plus IL-2. In contrast, B cells from the affected individual did not proliferate in response to IgM plus APRIL. For each sample, proliferation was measured in triplicate. Open bars, healthy control; filled bars, affected individual. WT, wild-type. (b) Detection of germline transcripts and circle transcripts after induced CSR. PBMCs were incubated with medium only, with IL-10 and CD40L, with IL-10 and APRIL or with IL-10 and BAFF. Expression of $I\gamma$ -C μ germline transcripts, $I\gamma$ -C μ circle transcripts and β -actin was determined after 2 d of incubation. The healthy control showed inducible CSR to IgG, the individual with TACI deficiency did not show an upregulated expression of germline transcripts or circle transcripts in response to stimulation with IL-10 and BAFF or with IL-10 and APRIL. (c) IgG secretion of B cells after induced CSR. PBMCs were incubated with medium only, with IL-10 and CD40L, with IL-10 and APRIL or with IL-10 and BAFF. IgG was measured in the culture supernatants after 7 d of incubation. The relative induction (compared with medium only) is depicted. Individuals with normal TACI secreted IgG in response to IL-10 and BAFF stimulation, but individuals with mutations of TACI did not. In an individual with CVID who does not carry any mutation of TACI, both CD40L and BAFF were able to induce IgG production (3.5- and 3.7-fold, respectively) as was, to a lesser degree, APRIL (1.3-fold); CVID (TACI wild-type).

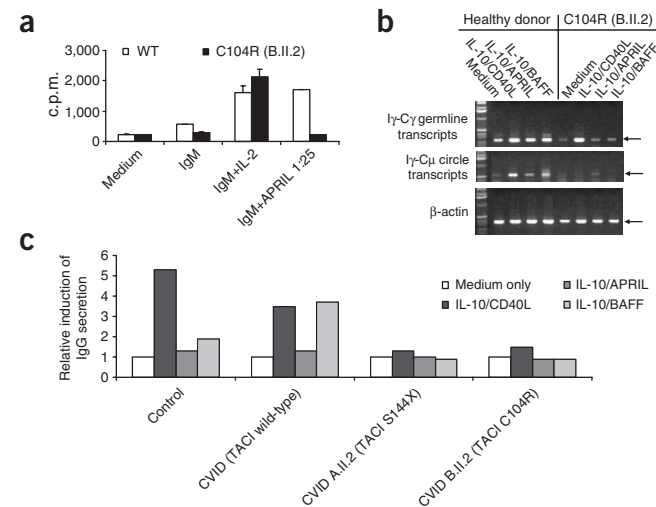


Table 1 Clinical summary of individuals with mutations in *TNFRSF13B*

Individual	Age	Sex	Immunodeficiency	IgG ^a	Autoimmunity	Lymphoproliferation	Mutation
A.II.1	68	Male	Hypogammaglobulinemia	4.1	None	Elevated B cells and CD8 ⁺ T cells	S144X (hom)
A.II.2	63	Male	CVID	2	None	Splenomegaly, lymphoid infiltration in the liver and gut	S144X (hom)
B.I.1	52	Male	Dysgammaglobulinemia	6.30	None	None	C104R (het)
B.I.2	50	Female	Dysgammaglobulinemia	9.54	Pos. ANA, thyroiditis	None	C104R (het)
B.II.1	22	Male	Hypogammaglobulinemia	5.43	None	Splenomegaly	C104R (het)
B.II.2	18	Male	CVID	4.2	None	Splenomegaly, tonsillar hyperplasia	C104R (hom)
C.I.2	79	Female	None	ND	None	None	A181E (het)
C.II.1	46 ^b	Male	CVID	<0.33	None	Splenomegaly	A181E (het)
C.II.2	43	Female	Sel. IgAD	18.7	None	None	A181E (het)
S1	65	Female	CVID	2.4	Pos. ANA, thyroiditis	Nodular lymphatic hyperplasia	C104R (het)
S2	73	Female	CVID	0.4	Pernicious anemia	Tonsillar hyperplasia	C104R (het)
S3	31	Male	CVID	2.5	None	None	A181E (het)
S4	34	Female	CVID	0.7	None	Splenomegaly, tonsillar hyperplasia	A181E (het)
S5	41	Female	CVID	2.3	None	None	A181E (het)
S6	41	Female	CVID	5.6	High titers of antibody to IgA	None	A181E (het)
S7	65	Female	CVID	0.5	None	Tonsillar hyperplasia	A181E (het)
S8	74 ^b	Female	CVID	1.0	None	None	A181E (hom)
S9	37	Male	CVID	0.15	None	Splenomegaly, peribronchial lymphatic hyperplasia	S194X (het)
S10	33	Female	CVID	2.52	Vitiligo, thyroiditis	Tonsillar hyperplasia	R202H (het)

^aIgG level at time of diagnosis, in g l⁻¹ (normal range is 7–16 g l⁻¹). ^bAge at death. het, heterozygous; hom, homozygous; ND, not done.

to CD40L, APRIL or BAFF after 7 d of incubation. In control cells, stimulation with CD40L and BAFF, in the presence of IL-10, induced IgG production (by 5.3- and 1.9-fold, respectively), whereas APRIL had only a moderate effect (1.3-fold induction; Fig. 3c). In cells from individuals with CVID, only CD40L slightly induced IgG production (by 1.3- and 1.5-fold in individuals A.II.2 and B.II.2, respectively), whereas stimulation with APRIL and BAFF had no effect on IgG production in either individual (Fig. 3c). Therefore, APRIL or BAFF can induce CSR from C_μ to C_γ and subsequent IgG production in B cells with normal TACI in a control or an individual with CVID, but neither APRIL nor BAFF can induce CSR and IgG production in TACI-deficient B cells.

Cellular phenotype in individuals with TACI deficiency

Individuals with mutations of TACI had a normal T-cell compartment, as evidenced by normal T-cell subsets and proliferative responses. Analysis of the peripheral B-cell compartment showed

normal total peripheral B-cell numbers for most of affected individuals, except individual A.II.2, who had undergone a splenectomy and had almost no circulating CD19⁺ cells (Fig. 4a), and his brother, who had not undergone a splenectomy but had slightly increased B-cell numbers (861 cells μl⁻¹; normal range is 100–500 cells μl⁻¹). The mutation in family A, leading to absent TACI protein, resembles the mouse TACI knockout most closely. In contrast, CD19⁺CD27⁺ memory B cell populations were diminished in most affected individuals, with a more severe decrease in the switched memory B-cell compartment (CD27⁺IgD⁻ B cells; Fig. 4a). Other than the loss of switched memory B cells, which is observed in ~75% of individuals with CVID²⁵, a distinct abnormal B-cell phenotype could not be observed in individuals with CVID and mutations in *TNFRSF13B*. This is in contrast to *Tnfrsf13b*^{-/-} mice¹⁵, which have an expanded population of circulating peripheral B cells.

Humoral immunity in individuals with TACI deficiency

Tnfrsf13b^{-/-} mice have low specific IgM and IgA antibody titers. After vaccination with T cell-independent antigens, their humoral response is severely impaired, with all immunoglobulin isotypes being affected¹³. In all individuals with CVID and TACI deficiency, IgM levels were decreased; IgM was undetectable in 6 of 13 individuals. IgA levels were low to undetectable in 10 of 13 individuals. In contrast to the murine model, total IgG at the time of diagnosis was low in all individuals, and six individuals were agammaglobulinemic (IgG ≤ 1.0 g l⁻¹; Table 1 and Fig. 4b). Ten of 13 individuals required continuous immunoglobulin substitution. The pronounced impairment of the switched isotypes IgG and IgA in individuals with TACI deficiency reflects the involvement of TACI and its ligands BAFF and APRIL in immunoglobulin CSR^{8,9} and is further underscored by the inability of B cells from these individuals to class-switch *in vitro* (Fig. 3b,c).

We also tested the sera of individuals with TACI deficiency for specific IgG antibodies against pneumococcal polysaccharide serotypes (PnPs) 1, 4, 5, 6B, 9V, 7, 14, 18, 19 and 23. As expected, individuals on regular Ig replacement therapy tested positive, but in individuals C.II.1, S1 and S4, all temporarily not on Ig therapy, PnPs-specific

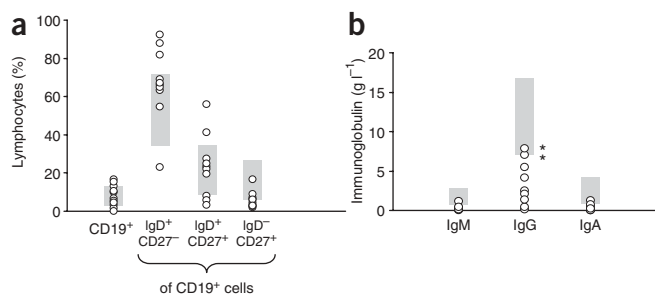


Figure 4 B-cell subpopulations and Ig levels in TACI deficiency. (a) CD19⁺ B cell numbers and IgD⁺CD27⁻, IgD⁺CD27⁺ and IgD⁻CD27⁺ subsets and (b) immunoglobulin levels at time of diagnosis in individuals with TACI deficiency. Each circle represents a single value from one individual; gray boxes indicate the normal range in age-matched healthy controls. Asterisks mark individuals undergoing immunoglobulin replacement therapy. B-cell subpopulations and Ig levels in TACI deficiency.

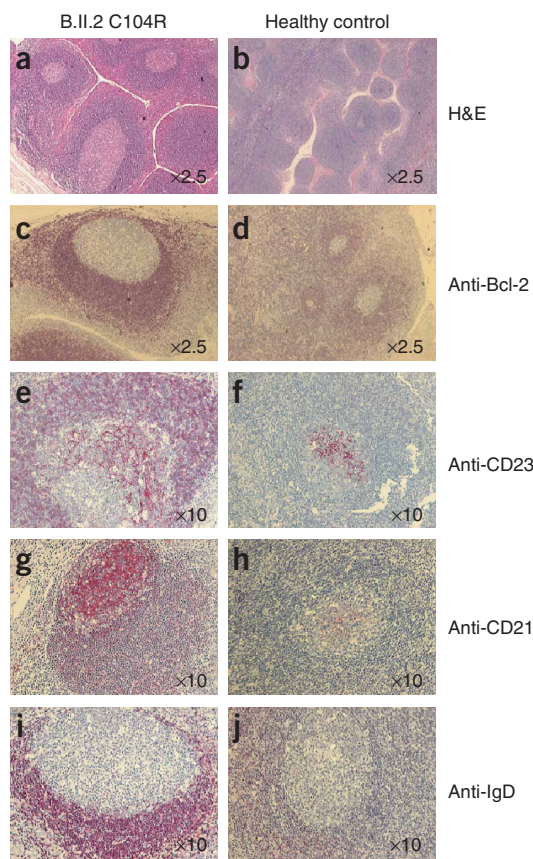


Figure 5 Tissue sections of a tonsil from an individual with TAC1 deficiency (a,c,e,g,i) compared with a normal control (b,d,f,h,j). (a,b) In identical fields, the follicles are enlarged and closely spaced (hematoxylin and eosin staining; H&E). (c,d) Prominent enlargement of secondary follicles in the hyperplastic tonsil compared with the normal tonsil, as evidenced by staining of the antiapoptotic protein Bcl-2. (e–h) The polarization of the germinal centers with a dark zone at the lower pole and a light zone containing CD23⁺ follicular dendritic cell meshworks towards the apical pole was more prominent in hyperplastic than in normal follicles. Immunolabeling for CD23 (e,f) and CD21 (g,h) highlighted a prominent scaffolding of the secondary follicles by follicular dendritic cell meshworks. Follicular dendritic cells were expanded in the enlarged apical mantle cuffs, which contained increased numbers of CD23⁺ and CD21⁺ lymphocyte subpopulations. (i,j) The enlarged mantle zones had an abundance of IgD⁺ B cells, which coexpressed IgM (data not shown).

lymphoid organs in TAC1-deficient mice¹⁵. The discrepancy between an enlarged mantle zone in the tonsil of this individual and the enlarged marginal zone previously reported¹⁵ may be due to the prominent marginal zone of the spleen in comparison to other lymphoid tissues, including tonsils.

DISCUSSION

Using a candidate gene approach in a cohort of 162 individuals affected by CVID, we identified three families and ten unrelated individuals with mutations in *TNFRSF13B*. The *TNFRSF13B* mutation spectrum is considerably more complex than that of the only other gene known to cause a typical CVID phenotype, *ICOS*; all *ICOS*-deficient individuals identified to date carry the same homozygous genomic deletion²⁰. Here, we report both homozygous and heterozygous mutations of TAC1 associated with a humoral immunodeficiency. In family B, the heterozygous mutation is associated with hypogammaglobulinemia, and the homozygous state is associated with the more severe CVID phenotype. In contrast, in family A the affected homozygous individuals have both mild and severe phenotypes (although the severity of the phenotype may be influenced by the splenectomy in individual A.II.2). For mutations in the heterozygote state, the clinical presentation ranges from unaffected (individual C.I.2) to severe CVID (individual C.II.1). The variable penetrance of TAC1 mutations in humans may reflect partial functional redundancy of the APRIL-BAFF-BAFFR-TAC1-BCMA system. In this regard, additional genetic alterations may contribute to the severity of individual phenotypes. Direct sequencing of exons encoding BAFF, BAFFR and BCMA in the individuals with TAC1 deficiency studied here detected no additional genetic alterations.

Several human diseases affecting the immune system and its inflammatory responses are caused by mutations in TNF receptor superfamily members (*TNFRSF*)^{27–29}. Mutations in *TNFRSF1A* cause an autosomal dominant inherited autoinflammatory condition called TNF-receptor associated periodic fever syndrome (TRAPS)²⁷; heterozygous mutations produce a dominant negative effect. Most of the observed mutations disrupt disulfide bridges in the cysteine-rich domains of *TNFRSF1A*, leading to impaired shedding of the extracellular domain from the cell surface²⁷.

Mutations in *CD40* (also called *TNFRSF5*) cause hyper-IgM syndrome type 3 (HIGM3). As with TAC1 deficiency, mutations of *CD40* affect immunoglobulin CSR²⁸. Notably, one of three individuals reported to have HIGM3 carries a mutation at a conserved cysteine residue.

Mutations in *FAS* (also called *TNFRSF6*) are responsible for a lymphoproliferative disorder with immunodeficiency: the autoimmune lymphoproliferative syndrome (ALPS, also called Canale-Smith

IgG antibodies were missing. Notably, individual A.II.1, who is not susceptible to recurrent infections and therefore not on Ig replacement therapy, had a normal basal level of PnPs antibodies. Because individual A.II.1 has no TAC1 protein on his B cells, PnPs-specific antibodies might be generated in the absence of TAC1.

Autoimmunity and lymphoproliferation in TAC1 deficiency

Individuals with CVID and mutations in *TNFRSF13B* had autoimmunity at a slightly higher frequency than did individuals with CVID in general. Signs of autoimmunity are usually present in ~20% of CVID patients¹⁶. In our cohort, 4 of 13 individuals (31%) showed autoimmune phenomena; splenomegaly was the most common sign of lymphoproliferation and was observed in 6 of 13 patients (Table 1).

Tissue typing showed a slightly higher frequency of the B8-DR3, DQ2 ancestral haplotype known to be associated with IgAD/CVID, indicative of a skewing in HLA distribution (Supplementary Table 1 online). More importantly, the DR15-DQ0602 haplotype, previously suggested to be highly protective against development of IgAD/CVID^{17,26}, was present in 4 of the 20 tested individuals. Therefore, although the number of individuals is too small to allow a definite conclusion, the overall pattern of HLA types in individuals with TAC1 deficiency seems to be different than that in individuals with idiopathic CVID.

Tonsil histology in an individual with TAC1 deficiency

The tonsil of individual B.II.2 contained markedly hyperplastic follicles, reflected by a lower number of secondary follicles per low-power field compared with a normal palatine tonsil (Fig. 5). The observation of hyperplasia of the B-cell region of the tonsil in this individual correlates well with the histology of the secondary

syndrome)²⁹. As reported here for TACI, both heterozygous and homozygous mutations of FAS may cause ALPS, with a more severe phenotype occurring in homozygous individuals. In addition, as described here for heterozygous mutations of TACI, individuals with heterozygous mutations of FAS also have a variable phenotype³⁰, thus serving as an example of dominant negative mutations³¹.

TACI, like FAS, requires ligand-induced trimerization (or even higher-order oligomerization) for signaling^{21,24,32}. The trimeric TRAF molecules acting downstream of numerous TNFRs, including TACI, have a high affinity for ligand-induced trimeric receptors but a very weak affinity for a single receptor³³. Recruitment of a single TACI mutant in a signaling complex can therefore compromise signaling by all remaining wild-type receptors, and poisoning of the complex could account for the effects of mutations S194X and R202H. Notably, the mutation R202H does not affect the TRAF binding sites but rather the region known to interact with CAML³⁴. The mutation A181E occurs in the transmembrane domain and may disturb the geometry of the intracellular portion of TACI; alternative explanations such as impaired partition of TACI in specialized membrane domains are also possible. The severely reduced TACI surface expression in individual B.II.2, homozygous with respect to the C104R mutation, can be explained either by defective transport of the mutant protein to the surface or by disruption of the 1A1 antibody epitope, which we mapped to amino acids 67–106 (P.S., unpublished data). In contrast, the normal TACI staining (Supplementary Fig. 1 online) and APRIL binding (data not shown) in individual S1, heterozygous with respect to the C104R mutation, raise the question of how this mutation acts in a dominant negative manner. As the inability of C104R mutant TACI to bind to APRIL should prevent the mutant protein from being incorporated into signaling complexes, a dominant negative effect is difficult to postulate. Alternative explanations may be a gene-dosage effect, which would be in contrast to the normal phenotype of *Tnfrsf13b*^{+/-} mice¹³, or the idea that mutant and wild-type TACI might be preassociated in a ligand-independent manner, as has been suggested for Fas³⁵.

Clinical presentation in individuals with TACI deficiency was dominated by humoral immunodeficiency, especially low IgM serum concentrations, lymphoproliferation and symptoms of autoimmunity. This triad of symptoms is mirrored in the *Tnfrsf13b*^{-/-} mouse model, but with different severity of the respective features: *Tnfrsf13b*^{-/-} mice predominantly show a severe lupus-like disease¹⁴, but none of the individuals with a mutation of TACI had any clinical features of systemic lupus erythematosus. The difference may be due to the inbred genetic background of the mice and the fact that most mutations in humans do not lead to complete loss of TACI (Supplementary Fig. 1 online). Although autoimmunity does not dominate the human phenotype, signs of lymphoproliferation were observed at a high frequency.

APRIL and BAFF induce CSR in B cells from both humans⁸ and mice⁹. In mice, *Tnfrsf13b*^{-/-} B cells do not synthesize IgG1, IgA and IgE in response to APRIL but are able to produce IgG1 and IgE in response to BAFF, suggesting that APRIL selectively mediates CSR to IgA through TACI whereas CSR to IgG1 and IgE may be mediated by BAFF through both TACI and BAFF-R⁹. In individuals with TACI deficiency, however, BAFF-induced CSR to IgG was also abolished. Our preliminary data further suggest that both APRIL- and BAFF-induced CSR to IgA was similarly impaired. As these individuals had normal binding of BAFF to BAFF-R, TACI probably has a key role in APRIL- and BAFF-induced CSR to both IgA and IgG in humans. This could potentially explain the observed difference, whereby most individuals with TACI deficiency had reduced serum levels of both

IgA and IgG, whereas *Tnfrsf13b*^{-/-} mice only had low serum IgA and IgM levels¹³. It is also worth noting that CD40L, another important ligand for induction of CSR, could induce I γ -C γ germline transcripts but did not induce IgG switching efficiently in individuals with TACI deficiency. This finding suggests that there may be cross-talk between the CD40-CD40L and APRIL-BAFF-TACI pathways, as reported previously⁸, although further analysis is required to delineate the underlying mechanism.

Because the human TACI-deficient phenotype is dominated by an antibody deficiency syndrome, rendering affected individuals susceptible to infections, the role of TACI in the humoral immune response must be taken into account when designing drugs aimed at interfering with the BAFF-APRIL-BAFFR-TACI-BCMA system, as previously suggested^{36,37}.

METHODS

Patients. At total of 162 individuals diagnosed with CVID according to the ESID/PAGID criteria were included in the study. Of these, 135 were sporadic cases and 27 were from multiplex families. Of those 27 families, 19 had an autosomal recessive pattern of inheritance. Seven of these families had known consanguinity. Seventy-two individuals originated from central Europe, 65 were from Scandinavia, 20 were from the UK and 5 were from Turkey. Thirteen of the families were selected from a collection of 101 multiplex CVID/IgA deficient families (including families cv22 and cv79)¹⁷ based in part on genetic linkage analysis evidence. Family A was selected for *TNFRSF13B* sequencing because it achieved both single and multipoint lod scores of +0.69 with markers flanking *TNFRSF13B*; most of the families evaluated by linkage analysis had negative multipoint scores in the vicinity of *TNFRSF13B*. Informed written consent was obtained from each individual before participation, under the internal ethics review board-approved clinical study protocol (ZERM, University Hospital Freiburg (#239/99) and 435/99 for L.H.).

Sequence analysis of *TNFRSF13B*. The primers used to amplify exons 1–5 of *TNFRSF13B* are listed in Supplementary Table 2 online. We sequenced PCR products with the PCR amplification primers. After gel electrophoresis on an ABI Prism377 DNA Sequencer (PE Applied Biosystems), we analyzed the data using the DNA Sequencing Analysis software version 3.4 (PE Applied Biosystems) and Sequencer version 3.4.1 (Gene Codes Corporation).

Analysis of the A181E variant of *TNFRSF13B* in population-based controls. We analyzed the A181E variant by MALDI-TOF SNP analysis in a population-based control cohort as described previously³⁸. We designed amplification and detection primers for the polymorphisms in question using the Spectro-Designer software (Sequenom). The PCR temperature profile started with 15 min of denaturation at 95 °C followed by 45 cycles of 94 °C for 30 s, 60 °C for 15 s and 72 °C for 15 s. A final elongation step of 72 °C for 5 min ended the program.

We carried out primer extension in a total volume of 9 μ l. After salt removal, we spotted ~10 nl of the samples onto Maldimatrix-containing SpectroCHIPS (Sequenom) using a nanodispenser (Robodesign). We analyzed the Spectro-CHIPS using an Autoflex MassARRAY mass spectrometer (Bruker Daltonics). Data were analyzed independently by two persons using the SpectroTyper software (Sequenom). We used the following primers to detect the A181E variant of *TNFRSF13B* in healthy controls: rsTAC11E, rsTAC11R and rsTAC11E (primer sequences are listed in Supplementary Table 2 online).

cDNA preparation and RT-PCR. We extracted total RNA from leukocytes, EBV-transformed B cells or enriched CD19⁺ B cells using the NucleoSpin RNA II kit (Macherey & Nagel) and then reverse-transcribed it using the ImProm reverse transcription system (Promega). We then amplified *TNFRSF13B* (TACI), *TNFRSF13C* (BAFFR), *TNFRSF17* (BCMA) and *CD19* as reference using the primers listed in Supplementary Table 2 online.

HLA typing. We carried out HLA-B, DR and DQ typing of individuals on genomic DNA using sequence-specific primers (HLA-B low resolution kit, DQ-DR SSP Combi Tray and DQB1*06 high resolution kit, Olerup SSP AB).

Isotype switching and Ig secretion by PBMCs. We cultured 1×10^6 PBMCs ml^{-1} isolated from affected individuals and controls, either with no treatment or stimulated with IL-10 (10 ng ml^{-1} , R&D Systems) and CD40L (300 ng ml^{-1} , a gift from Immunex, Seattle, USA), with IL-10 and April (300 ng ml^{-1} , R&D Systems) or with IL-10 and BAFF (300 ng ml^{-1} , R&D Systems). We collected cells after 48 h and collected culture supernatants at day 7 for IgG determination.

We amplified the germline transcripts using $I\gamma$ -consensus and $C\gamma$ -consensus primers and the circle transcripts using $I\gamma$ -consensus and $C\mu$ -antisense primers. The primers sequences are listed in **Supplementary Table 2** online. Amplification was done in 32 ($I\gamma$ - $C\gamma$) or 40 ($I\gamma$ - $C\mu$) cycles, each cycle consisting of 94°C for 50 s, 62°C (65°C for $I\gamma$ - $C\mu$) for 50 s and 72°C for 1 min. We monitored the integrity of RNA and cDNA synthesis by amplification of β -actin mRNA³⁹. We determined IgG concentrations in cell culture supernatants using standard ELISA procedures and using rabbit antibody to human IgG as capture and alkaline phosphatase-conjugated rabbit antibody to human IgG for detection (both from DAKO). We used human serum with a known concentration of IgG as standard.

FACS staining of peripheral B cells. We isolated PBMCs by Ficoll density gradient centrifugation and stained them with quadruple combinations of monoclonal antibodies: rat antibody to human TACI (1A1; Abcam or Alexis Biochemicals) or goat antibody to human BAFFR (R&D Systems) followed by phycoerythrin-labeled appropriate secondary antibodies or phycoerythrin-labeled isotype controls together with CD19-PC7 (J4.119; Beckman Coulter), CD27-fluorescein isothiocyanate (M-T271; Dako) and goat F(ab)₂ antibody to human IgD-Cy5 (Bioszol) or rabbit antibody to human IgM-Cy5 (Dianova). We acquired at least 10^4 live cells, gated according to their forward and side scatters, and analyzed them on a FACSCalibur using CELLQuest software (Becton Dickinson). We stained dead cells with propidium iodide and excluded them by electronic gating.

Binding of FLAG-APRIL and FLAG-BAFF. We produced FLAG-ACRP-APRIL (amino acids 98–233), FLAG-APRIL (amino acids 93–233), FLAG-ACRP-BAFF (amino acids 137–285) and Fc-APRIL (amino acids 98–233) in supernatants of 293T cells as described^{24,32}. We stained 10^6 EBV-transformed cells with 10–50 ng of FLAG-ACRP-APRIL or FLAG-ACRP-BAFF in the presence of 0.1 μl of heparin (Liquemin, Roche Pharma) and revealed staining with antibody to FLAG M2 (Sigma) and phycoerythrin-labeled goat antibody to mouse (Caltag). We assessed the specificity of binding of FLAG-ACRP-APRIL to EBV-transformed cells by preincubating cells with Fc-APRIL (10 μl of 20-fold concentrated supernatants, corresponding to $\sim 0.5 \mu\text{g}$ of Fc-APRIL) and then staining them with FLAG-ACRP-APRIL as described above. Under these conditions, specific staining of FLAG-ACRP-APRIL on TACI-transfected 293T cells or on the TACI-positive cell line IM9 was efficiently competed (data not shown).

Proliferation of purified B cells to IgM/APRIL mediated costimulation. We isolated PBMCs from EDTA-blood by Ficoll-Hypaque density gradient centrifugation (Biochrom) and cultured them in RPMI 1640 medium supplemented with penicillin, streptomycin, L-glutamine and 10% heat-inactivated fetal calf serum. We negatively selected CD19⁺ B cells with the human B cell isolation kit (Miltenyi Biotec) to a purity of >90% and then stimulated them in triplicate with a goat F(ab)₂ fragment antibody to human IgM ($12.5 \mu\text{g ml}^{-1}$, ICN) alone or in combination with 20 U ml^{-1} IL-2 (Biotest) or a 1/25 dilution of supernatant from 293T cells expressing soluble FLAG-APRIL in the presence of $1 \mu\text{g ml}^{-1}$ antibody to FLAG M2. Alternatively, we stimulated negatively isolated B cells with $12.5 \mu\text{g ml}^{-1}$ antibody to IgM (ICN), $12.5 \mu\text{g ml}^{-1}$ antibody to IgM plus 20 U ml^{-1} IL-2 (Biotest), $5 \mu\text{g ml}^{-1}$ antibody to CD40 alone (R&D Systems) and $5 \mu\text{g ml}^{-1}$ antibody to CD40 plus 20 U ml^{-1} IL-4 (Roche). We cultured 50,000 cells per well in 96-well round-bottom plates for 96 h with [³H] thymidine or BrdU (Roche) added for the last 16 h. We collected cells and quantified incorporated radioactivity with a Matrix 96 beta counter (Canberra Packard) or determined proliferation using the BrdU cell proliferation kit (Roche) in accordance with the manufacturer's instructions.

Immunohistochemistry. In addition to conventional histological stains (hematoxylin and eosin, Giemsa and periodic acid Schiff), we immunostained paraffin-embedded sections of the formalin-fixed tonsil biopsy of individual B.II.2 and a clinically normal control tonsil after heat-mediated antigen retrieval. We obtained the primary antibodies from DakoCytomation: CD20 (clone L26), CD3 (clone F7.2.38), CD4 (clone MT310), CD5 (clone CD5/54/F6), CD8 (clone C8/144B), CD10 (clone SS2/36), CD21 (clone 1F8), CD23 (clone MHM6), CD30 (clone Ber-H2), CD43 (clone DF-T1), CD68 (clone PGM1), CD79a (clone JCB117), Ki67 (clone MIB-1), cyclin D1 (clone DCS-6), BCL2 oncoprotein (clone 124), BCL6 protein (clone PG-B6p), multiple myeloma oncogene1/interferon regulatory factor 4 (clone1/IRF4) IgA (clone 6E2C1), IgD (clone IgD26), IgG (clone A57H), IgM (clone R1/69) and polyclonal anti- κ and λ . We visualized the antibodies using the ChemMate Detection Kit, AP/RED (DakoCytomation).

Genetic linkage analysis of available pedigrees. Phenotypes and genotypes from a genome scan were available for 101 multiplex IgA deficiency families, which had been previously analyzed by model-free linkage analysis methods to identify and finely map the *IGAD1* locus on chromosome 6 (ref. 26). Of these families, 43 include at least one individual with the more severe CVID phenotype. The available individuals included the three children in family A and individuals C.I.2, C.II.1 and C.II.2. Because we were seeking monogenic cases, we reanalyzed the pedigree data using dominant and recessive penetrance models. We computed lod scores with the FASTLINK software package^{40,41}. Marker allele frequencies were retained from the previous study. We set the disease allele frequency to 0.001 for the dominant analysis and 0.01 for the recessive analysis. Individuals with CVID were not allowed to be phenocopies, whereas individuals with less severe (and more common) hypogammaglobulinemia were assigned a phenocopy rate of 0.01. Unaffected individuals who were phenotyped as such were assigned a 0.25 conditional probability of carrying a disease-associated genotype, even though they are unaffected (which is called 75% penetrance in LINKAGE notation). The dominant inheritance in family C is not detectable because in 2000 individual C.I.2 was classified as 'unaffected'¹⁷.

TNFRSF13B is located $\sim 16.8 \text{ Mb}$ from 17ptel on human genome build 35.1 flanked by markers *D17S799* (13.1 Mb) and *D17S798* (28.1 Mb), which are separated by $\sim 20 \text{ cM}$ in genetic map units. We sought families with positive single-marker and multipoint lod scores.

GenBank accession number. *TNFRSF13B* mRNA, NM 012452.

Note: Supplementary information is available on the Nature Genetics website.

ACKNOWLEDGMENTS

We thank H. Eibel and K. Warnatz for advice; J. Deimel, R. Dräger, B. Ferry, M. Ibrahim, K. Ingold, J. Pfannstiel, A. Rump, A. Tardivel, M. Vogel, S. Workman and C. Woellner for assistance; A.-M. Eades-Perner, J. Puck and U. Walker for critically reading the manuscript; U. Hannelius and J. Kere for sharing their material and method for population-based screening; E. Walther for providing the tonsil specimens; and I. Vorechovský for providing the genotypes of CVID families. This research was supported by grants from the Deutsche Forschungsgemeinschaft, the Swedish research council and the European Union.

COMPETING INTERESTS STATEMENT

The authors declare that they have no competing financial interests.

Received 7 February; accepted 16 May 2005

Published online at <http://www.nature.com/naturegenetics/>

- Mackay, F. & Ambrose, C. The TNF family members BAFF and APRIL: the growing complexity. *Cytokine Growth Factor Rev.* **14**, 311–324 (2003).
- Mackay, F., Schneider, P., Rennert, P. & Browning, J. BAFF AND APRIL: a tutorial on B cell survival. *Annu. Rev. Immunol.* **21**, 231–264 (2003).
- Ng, L.G. *et al.* B cell-activating factor belonging to the TNF family (BAFF)-R is the principal BAFF receptor facilitating BAFF costimulation of circulating T and B cells. *J. Immunol.* **173**, 807–817 (2004).
- Avery, D. *et al.* BAFF selectively enhances the survival of plasmablasts generated from activated human memory B cells. *J. Clin. Invest.* **112**, 286–297 (2003).
- Wu, Y. *et al.* Tumor necrosis factor (TNF) receptor superfamily member TACI is a high affinity receptor for TNF family members APRIL and BlyS 275. *J. Biol. Chem.* **275**, 35478–35485 (2000).
- Varfolomeev, E. *et al.* APRIL-deficient mice have normal immune system development. *Mol. Cell. Biol.* **24**, 997–1006 (2004).

7. Castigli, E. *et al.* Impaired IgA class switching in APRIL-deficient mice. *Proc. Natl. Acad. Sci. USA* **101**, 3903–3908 (2004).
8. Litinskiy, M.B. *et al.* DCs induce CD40-independent immunoglobulin class switching through BLyS and APRIL. *Nat. Immunol.* **3**, 822–829 (2002).
9. Castigli, E. *et al.* TACI and BAFF-R mediate isotype switching in B cells. *J. Exp. Med.* **201**, 35–39 (2005).
10. Schiemann, B. *et al.* An essential role for BAFF in the normal development of B cells through a BCMA-independent pathway. *Science* **293**, 2111–2114 (2001).
11. Thompson, J.S. *et al.* BAFF-R a newly identified TNF receptor that specifically interacts with BAFF. *Science* **293**, 2108–2111 (2001).
12. Shulga-Morskaya, S. *et al.* B cell-activating factor belonging to the TNF family acts through separate receptors to support B cell survival and T cell-independent antibody formation. *J. Immunol.* **173**, 2331–2341 (2004).
13. von Bülow, G.U., van Deursen, J.M. & Bram, R.J. Regulation of the T-independent humoral response by TACI. *Immunity* **14**, 573–582 (2001).
14. Seshasayee, B. *et al.* Loss of TACI causes fatal lymphoproliferation and autoimmunity, establishing TACI as an inhibitory BLyS receptor. *Immunity* **18**, 279–288 (2003).
15. Yan, M. *et al.* Activation and accumulation of B cells in TACI-deficient mice. *Nat. Immunol.* **2**, 638–643 (2001).
16. Cunningham-Rundles, C. & Bodian, C. Common variable immunodeficiency: clinical and immunological features of 248 patients. *Clin. Immunol.* **92**, 34–48 (1999).
17. Vořechovský, I., Cullen, M., Carrington, M., Hammarström, L. & Webster, A.D.B. Fine mapping of *IGAD1* in IgA deficiency and common variable immunodeficiency: Identification and characterization of haplotypes shared by affected members of 101 multiple-case families. *J. Immunol.* **164**, 4408–4416 (2000).
18. Burrows, P.D. & Cooper, M.D. IgA deficiency. *Adv. Immunol.* **65**, 245–276 (1997).
19. Grimbacher, B. *et al.* Homozygous loss of ICOS is associated with adult-onset common variable immunodeficiency. *Nat. Immunol.* **4**, 261–268 (2003).
20. Salzer, U. *et al.* ICOS deficiency in patients with common variable immunodeficiency. *Clin. Immunol.* **113**, 234–240 (2004).
21. Hymowitz, S.G. *et al.* Structures of APRIL-receptor complexes: Like BCMA, TACI employs only a single cysteine-rich domain for high-affinity ligand binding. *J. Biol. Chem.* **280**, 7218–7227 (2004).
22. Riva, A. & Kohane, I.S. SNPper: retrieval and analysis of human SNPs. *Bioinformatics* **18**, 1681–1685 (2002).
23. Ng, P.C. & Henikoff, S. SIFT: Predicting amino acid changes that affect protein function. *Nucleic Acids Res.* **31**, 3812–3814 (2003).
24. Ingold, K. *et al.* Identification of proteoglycans as APRIL-specific binding partners. *J. Exp. Med.* **201**, 1375–1383 (2005).
25. Warnatz, K. *et al.* Severe deficiency of switched memory B cells (CD27⁺IgM⁺IgD⁻) in subgroups of patients with common variable immunodeficiency: a new approach to classify a heterogeneous disease. *Blood* **99**, 1544–1551 (2002).
26. Kralovicova, J., Hammarström, L., Plebani, A., Webster, A.D.B. & Vorechovsky, I. Fine-scale mapping at *IGAD1* and genome-wide genetic linkage analysis implicate *HLA-DQ/DR* as a major susceptibility locus in selective IgA deficiency and common variable immunodeficiency. *J. Immunol.* **170**, 2765–2775 (2003).
27. McDermott, M.F. *et al.* Germline mutations in the extracellular domains of the 55 kDa TNF receptor, TNFR1, define a family of dominantly inherited autoinflammatory syndromes. *Cell* **97**, 133–144 (1999).
28. Ferrari, S. *et al.* Mutations of CD40 gene cause an autosomal recessive form of immunodeficiency with hyper IgM. *Proc. Natl. Acad. Sci. USA* **98**, 12614–12619 (2001).
29. Rieux-Laucat, F. *et al.* Mutations in Fas associated with human lymphoproliferative syndrome and autoimmunity. *Science* **268**, 1347–1349 (1995).
30. Infante, A.J. *et al.* The clinical spectrum in a large kindred with autoimmune lymphoproliferative syndrome caused by a Fas mutation that impairs lymphocyte apoptosis. *J. Pediatr.* **133**, 629–633 (1998).
31. Fisher, G.H. *et al.* Dominant interfering Fas gene mutations impair apoptosis in a human autoimmune lymphoproliferative syndrome. *Cell* **81**, 935–946 (1995).
32. Holler, N. *et al.* Two adjacent trimeric Fas ligands are required for Fas signaling and formation of a death-inducing signaling complex. *Mol. Cell. Biol.* **23**, 1428–1440 (2003).
33. Wu, H. Assembly of post-receptor signaling complexes for the tumor necrosis factor receptor superfamily. *Adv. Protein Chem.* **68**, 225–279 (2004).
34. Xia, X.Z. *et al.* TACI is a TRAF-interacting receptor for TALL-1, a tumor necrosis factor family member involved in B cell regulation. *J. Exp. Med.* **192**, 137–143 (2000).
35. Siegel, R.M. *et al.* Fas preassociation required for apoptosis signaling and dominant inhibition by pathogenic mutations. *Science* **288**, 2354–2357 (2000).
36. Gross, J.A. *et al.* TACI-Ig neutralizes molecules critical for B cell development and autoimmune disease. Impaired B cell maturation in mice lacking BLyS. *Immunity* **15**, 289–302 (2001).
37. Baker, K.P. *et al.* Generation and characterization of LymphoStat-B, a human monoclonal antibody that antagonizes the bioactivities of B Lymphocyte Stimulator. *Arthritis Rheum.* **48**, 3253–3265 (2003).
38. Hannelius, U. *et al.* Phenylketonuria screening registry as a resource for population genetic studies. *J. Med. Genet.* (in the press).
39. Pan, Q., Lindersson, Y., Sideras, P. & Hammarström, L. Structural analysis of human $\gamma 3$ intervening regions and switch regions: implication for the low frequency of switching in IgG3-deficient patients. *Eur. J. Immunol.* **27**, 2920–2926 (1997).
40. Lathrop, G.M., Lalouel, J.M., Julier, C. & Ott, J. Strategies for multilocus analysis in humans. *Proc. Natl. Acad. Sci. USA* **81**, 3443–3446 (1984).
41. Cottingham, R.W. Jr., Idury, R.M. & Schäffer, A.A. Faster sequential genetic linkage computations. *Am. J. Hum. Genet.* **53**, 252–263 (1993).